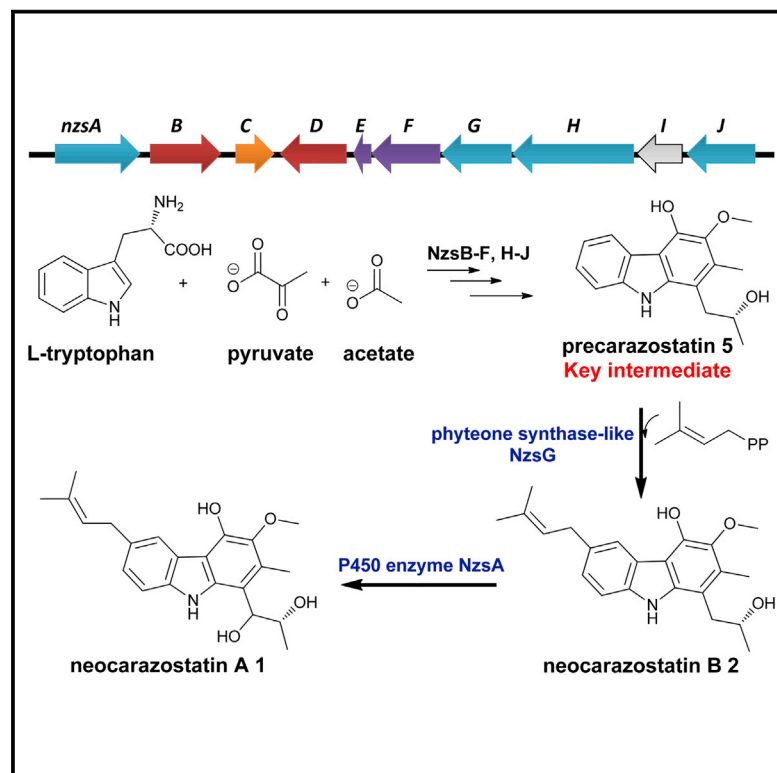# Chemistry & Biology

# Biosynthesis of Neocarazostatin A Reveals the Sequential Carbazole Prenylation and Hydroxylation in the Tailoring Steps

## Graphical Abstract

## Authors

Sheng Huang,
Somayah Sameer Elsayed,
Meinan Lv, ..., Zixin Deng, Yi Yu,
Hai Deng

## Correspondence

h.deng@abdn.ac.uk (H.D.),
yu_yi@whu.edu.cn (Y.Y.)

## In Brief

Huang et al. identified the gene cluster directing the biosynthesis of neocarazostatin A, characterized two new enzymes responsible for the late stage of the biosynthesis, and reconstituted in vitro the biotransformation from the biosynthetic intermediate to neocarazostatin A.

## Highlights

- The biosynthetic gene cluster of neocarazostatin A was identified

- A new type of carbazole prenyltransferases, NzsG, was characterized

- The P450 enzyme NzsA catalyzing the last step of the biosynthesis was identified

- The biotransformation in the late stage of the biosynthesis was reconstituted

## Accession Numbers

KP657980

CellPress

**Chemistry & Biology**

# Article

CellPress

# Biosynthesis of Neocarazostatin A Reveals the Sequential Carbazole Prenylation and Hydroxylation in the Tailoring Steps

Sheng Huang,[1] Somayah Sameer Elsayed,[2] Meinan Lv,[1] Jioji Tabudravu,[2] Mostafa E. Rateb,[2,4] Roland Gyampoh,[3] Kwaku Kyeremeh,[3] Rainer Ebel,[2] Marcel Jaspars,[2] Zixin Deng,[1] Yi Yu,[1,*] and Hai Deng[2,*]

[1]Key Laboratory of Combinatory Biosynthesis and Drug Discovery (Ministry of Education), School of Pharmaceutical Sciences, Wuhan University, 185 East Lake Road, Wuhan 430071, P.R. China
[2]Department of Chemistry, University of Aberdeen, Aberdeen AB24 3UE, UK
[3]Department of Chemistry, University of Ghana, P.O. Box LG56, Legon-Accra, Ghana
[4]Pharmacognosy Department, School of Pharmacy, Beni-Suef University, Beni-Suef 32514, Egypt
*Correspondence: h.deng@abdn.ac.uk (H.D.), yu_yi@whu.edu.cn (Y.Y.)
http://dx.doi.org/10.1016/j.chembiol.2015.10.012

## SUMMARY

**Neocarazostatin A (NZS) is a bacterial alkaloid with promising bioactivities against free radicals, featuring a tricyclic carbazole nucleus with a prenyl moiety at C-6 of the carbazole ring. Here, we report the discovery and characterization of the biosynthetic pathway of NZS through genome mining and gene inactivation. The in vitro assays characterized two enzymes: NzsA is a P450 hydroxylase and NzsG is a new phytoene-synthase-like prenyltransferase (PTase). This is the first reported native PTase that specifically acts on the carbazole nucleus. Finally, our in vitro reconstituted experiment demonstrated a coupled reaction catalyzed by NzsG and NzsA tailoring the NZS biosynthesis.**

## INTRODUCTION

Carbazoles consist of a tricyclic nucleus with two benzene rings flanking a pyrrole ring. Most of the known naturally occurring carbazole alkaloids contain an annulated ring or ring system in both benzene rings and were isolated from higher plants and fungi, which display a broad range of biological properties such as anticancer, antibacterial, antiviral, and antiplasmodial activities (Knölker and Reddy, 2002). At present, the biosynthesis of plant carbazole metabolites is not fully understood (Schmidt et al., 2012). The most widely accepted hypothesis is that the nucleus of carbazole alkaloids from higher plants may derive from anthranilic acids and prenyl pyrophosphate (Schmidt et al., 2012).

In contrast to widespread carbazole alkaloids from higher plants and fungi, bacterial carbazole metabolites are much less common. The first class of bacterial carbazoles are indolo[2,3-a]pyrrolo[3,4-c] carbazoles, representatives of which include staurosporine (Meksuriyen and Cordell, 1988) and rebeccamycin (Pearce et al., 1988), and the second class are indolosesquiterpenes, representatives of which are oridamycins (Takada et al., 2010) and xiamycins (Ding et al., 2010, 2011). The bio-origins of

both types of carbazole-containing metabolites have been well established in the last decade (Howard-Jones and Walsh, 2006; Xu et al., 2012; Li et al., 2012, 2015; Baunach et al., 2015). The third type of carbazoles, however, consist of a simple tricyclic ring system with aliphatic side chains, including carquinostatins, carazostatin, carbazoquinocins, carbazomycin, (S)-streptoverticillin, and neocarazostatins (Feng et al., 2007; Kato et al., 1989, 1991; Ruanpanun et al., 2011; Sakano and Nakamura, 1980; Shin-ya et al., 1993, 1997; Tanaka et al., 1995) (Figure 1). Generally this group of bacterial carbazoles can act as free radical scavengers and exhibit potent neuronal cell-protecting activity (Schmidt et al., 2012). Free radicals play a key role in the initiation of a variety of diseases such as cerebral and myocardial ischemia, arteriosclerosis, inflammation, rheumatism, and cancer. Antioxidants, acting as free radical scavengers, can act as protecting substances against damage caused by free radicals (Palinski et al., 1989). In this respect, free radical scavenging compounds are being extensively investigated as potential drug leads (Schmidt et al., 2012). Due to their pharmacological potential as cell-protecting agents, there has been considerable interest among medicinal chemists to develop this class of molecules (Choshi et al., 1997; Czerwonka et al., 2006; Rawat and Wulff, 2004; Shin-ya and Ogasawara, 1996). The biosynthetic pathways of this group of bacterial carbazoles have not been reported, although feeding experiments confirmed that L-tryptophan, pyruvate, and acetate provide the carbazole nucleus (Kaneda et al., 1990; Orihara et al., 1997; Yamasaki et al., 1983) (Figure S1A).

In our screening program to discover novel natural products from the soil bacterium *Streptomyces* sp. MA37 (Deng et al., 2014; Huang et al., 2015; Ma et al., 2015), neocarazostatin A **1** was isolated from this strain (Figures S1B–S1G). Neocarazostatins A–C (Figure 1) were originally discovered from the culture of *Streptomyces* sp. GP38 in 1991 (Kato et al., 1991). The neocarazostatins exhibited a strong inhibitory effect on the free radical-induced lipid peroxidation in rat brain homogenate. The $IC_{50}$ values of the neocarazostatins for inhibition of lipid peroxidation were considerably lower than those of the free radical scavenger butylhydroxytoluene and the brain-protective agent flunarizine (Kato et al., 1991).

In this study, we report the actinobacterial biosynthetic gene cluster for the biosynthesis of NZS. Two enzymes, NzsA and
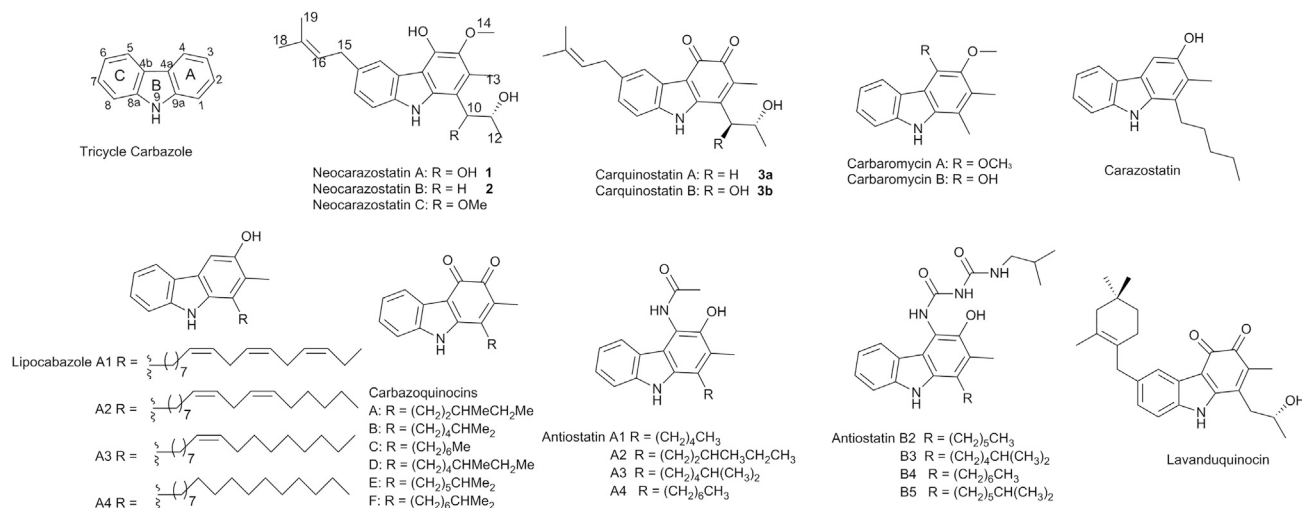
**Figure 1. Chemical Structures of Common Tricyclic Carbazole Alkaloids from Bacteria**

NzsG, were biochemically characterized. NzsA is a P450 hydroxylase and NzsG is a phytoene-synthase-like (PSL) prenyltransferase, a PSL protein that catalyzes the prenylation of carbazole. Finally, we reconstituted in vitro the last two steps of the pathway to NZS using purified recombinant enzymes.

## RESULTS

### Identification of the *nzs* Gene Cluster

NZS **1** possesses a prenyl group at C-6 on the indole ring. Initially, a homolog search of bacterial indole prenyltransferases was conducted. IptA from *Streptomyces* sp. SN-593 has been shown to be a 6-dimethyl-allyl (DMAL)-L-tryptophan synthase which is involved in the biosynthesis of 6-DMAL-3-carbaldehyde (Takahashi et al., 2010). Although IptA homologs appeared to be widely spread in the *Streptomyces* genome, to our surprise, a BLAST (Basic Local Alignment Search Tool) search of the annotated genome of MA37 in the RAST server (Aziz et al., 2008) yielded no open reading frames (ORFs) with any obvious sequence identity to IptA in MA37.

Previous labeling studies established that indole pyruvate originating from L-tryptophan is likely to contribute rings B and C plus the intact C2 unit of C-3 and C-4 of ring A in the biosynthesis of carquinostatin B **3b** (Figure S1A) (Kato et al., 1991), a structurally close analog of **1** (Figure 1). The incorporation of pyruvate in secondary metabolism can also be observed in the biosynthesis of sugars containing a two-carbon branched chain, such as antibiotic natural products, yersiniose A from the Gram-negative bacterium *Yersinia pseudotuberculosis* (Chen et al., 1998), aldgamycin E from *Saccharothrix* SA 103 (Ellestad et al., 1967), and presumably tianchimycin B from *Saccharothrix xinjiangensis* (Wang et al., 2013). An in vitro assay indicated that the gene product YerE is a thiamine pyrophosphate (ThDP)-dependent enzyme, responsible for the C-C bond formation between 3-ketosugar and pyruvate during the biosynthesis of yersiniose A (Chen et al., 1998; Lehwald et al., 2010). We performed a homolog search of YerE in MA37, resulting in identification of an ORF, annotated as a ThDP-dependent enzyme (NzsH)

(Figure 2A and Table 1), which shows moderate sequence identity (27%) to YerE.

Analysis of the genes in close proximity of *nzsH* allowed us to retrieve a candidate gene cluster (*nzs*) spanning approximately 17.8 kb (Figure 2A and Table 1). The *nzs* cluster possesses ten ORFs, nine of which (NzsA-H and J) can be assigned catalytic functions (Table 1). A BLAST search of NzsI indicated that it belongs to a small group of hypothetical proteins with no obvious catalytic function. Genes beyond this region are highly conserved in the chromosomes of other non-NZS producing *Streptomyces* strains such as *Streptomyces griseus*, *Streptomyces avermitilis*, and *Streptomyces coelicolor* (Figure S2A). Thus, we propose that these ten *orf*s define the boundaries of the *nzs* cluster.

### In Vivo Experiments Confirmed that the Candidate Gene Cluster Directs the Biosynthesis of NZS 1

To confirm the identity of the *nzs* cluster we performed gene disruption, and ten different mutants (Δ*nzsA–J*) were generated (Figures S2B–S2L). High-performance liquid chromatography (HPLC) analysis of the extracts from these mutants demonstrated that inactivation of *nzsE*, *F* and *nzsH–J* completely abolished the NZS production (Figure 2B), suggesting that these five ORFs are essential for the biosynthesis of **1**. Inactivation of *nzsB–D*, encoding anthranilate phosphoribosyltransferase, isopentenyl diphosphate (IPP) isomerase, and aromatic aminotransferase, respectively, resulted in only slightly decreased production of **1** (Figure 2B **5–8**). In accordance with these findings, bioinformatics analyses of the draft genome sequence of the MA37 revealed the presence of several other gene copies with predicted functions similar to NzsB–D, suggesting the cross-complementation roles played by these genes.

Gene disruption of *nzsG* completely abolished the production of **1** but resulted in accumulation of two new metabolites in the culture of the Δ*nzsG* mutant (Figure 2B **4**). Subsequently, fermentation and chemical isolation afforded two pure compounds, **4** (7 mg) and **5** (4.3 mg) (Figure 3). The structures of **4** and **5** were established by the inspection of high-resolution
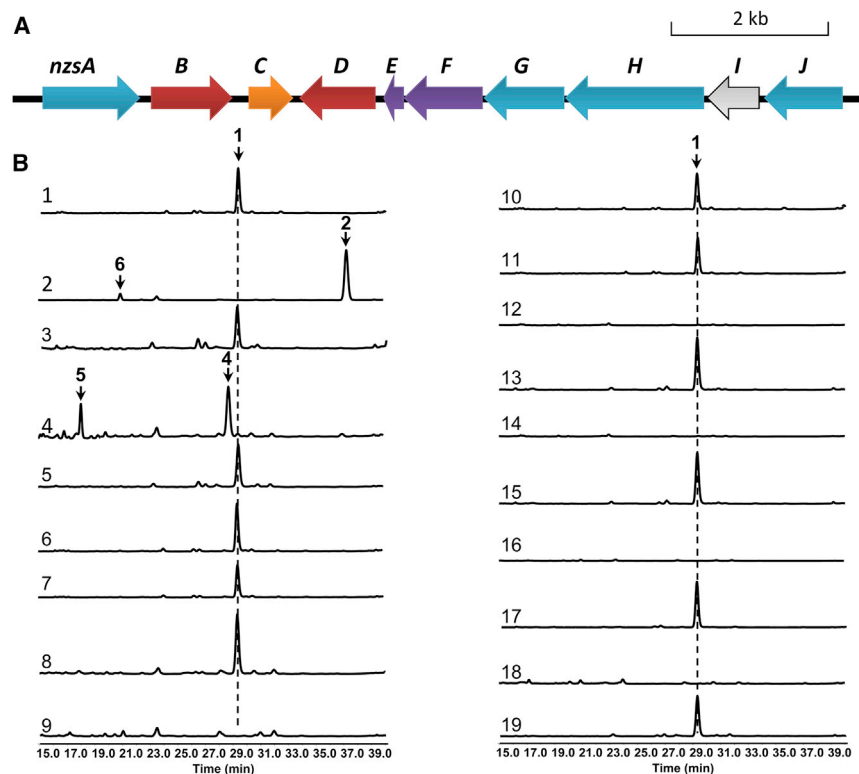
**Figure 2. Production of NZS by *Streptomyces* sp. MA37 and Mutants**

(A) Genetic organization of the *nzs* biosynthetic gene cluster. Blue: the genes putatively involved in the biosynthesis of 1. Red: genes involved in the biosynthesis of indole-3-pyruvate precursor. Yellow: genes involved in the biosynthesis of DMAPP precursor. Purple: genes putatively involved in the polyketide synthase biosynthesis. Gray: gene with unknown function.

(B) HPLC analyses (UV at 247 nm) of extracts from the *Streptomyces* sp. MA37 wild-type and mutant strains. **1** and **10**: wild-type strain; **2**: WDY633 (Δ*nzsA* mutant); **3**: WDY634 (Δ*nzsA* complementation mutant); **4**: WDY638 (Δ*nzsG* mutant); **5**: WDY639 (Δ*nzsG* complementation mutant); **6**: WDY640 (Δ*nzsB* mutant); **7**: WDY641 (Δ*nzsC* mutant); **8**: WDY642 (Δ*nzsD* mutant); **9**: WDY644 (Δ*nzsE* mutant); **11**: WDY645 (Δ*nzsE* complementation mutant); **12**: WDY646 (Δ*nzsF* mutant); **13**: WDY647 (Δ*nzsF* complementation mutant); **14**: WDY630 (Δ*nzsH* mutant); **15**: WDY631 (Δ*nzsH* complementation mutant); **16**: WDY648 (Δ*nzsI* mutant); **17**: WDY649 (Δ*nzsI* complementation mutant); **18**: WDY635 (Δ*nzsJ* mutant); **19**: WDY636 (Δ*nzsJ* complementation mutant).

electrospray ionization mass spectrometry (HR-ESIMS) and 1D and 2D nuclear magnetic resonance (NMR) spectral data, and by comparison of the NMR spectral data with those of **1** (Tables S4 and S5; Figures S3A–S3F, and S3M–S3R). Although compound **4** has chemical shifts in NMR spectra identical to the known carbazole metabolite, (S)-streptoverticillin, comparison of the values of the optical rotation of **4** with the ones of (S)-streptoverticillin and its non-natural enantiomer (R)-streptoverticillin (Thomas et al., 2011) indicated that **4** actually is (R)-streptoverticillin. Compound **5** is a new carbazole intermediate, which was named as precarazostatin. Both **4** and **5** lack prenyl substitution at C-6, suggesting that NzsG may be responsible for the prenylation at C-6 of the carbazole nucleus.

HPLC analysis also showed that, while the production of **1** was lost in the culture of the Δ*nzsA* mutant, two new metabolites, **2** and **6**, were accumulated (Figure 2B 2). Fermentation and isolation, followed by analyses of HR-ESIMS and 1D and 2D NMR spectral and optical rotation data, established that one metabolite is a known carbazole metabolite, neocarazostatin B **2** (Figures 3 and S3G–S3R), a close derivative of **1**, suggesting that NzsA may be responsible for the installation of the hydroxyl group at C-11 of **2** to generate **1**. The structure of compound **6** was determined as a new epoxy derivative of **2** on the basis of HR-ESIMS and 1D and 2D NMR analyses, which clearly indicated the replacement of $\Delta^{16,17}$ in **2** with an epoxy ring (Figures 3, S3S–S3X).

## Biochemical Assay Demonstrated that NzsG Is a New Prenyltransferase that Specifically Acts on 5

Given that **4** and **5** are not further metabolized in the Δ*nzsG* mutant, it was envisaged that they may be immediate substrates of NzsG. Bioinformatics analysis revealed that NzsG shares high sequence

identity (60%–65%) with only three hypothetical proteins from *Streptomyces* but has 25%–40% similarity to a large family of putative phytoene synthases from actinomycetes. It also possesses a characteristic DDxxD motif, which is essential for binding prenyl diphosphate via metal ions (Liang et al., 2002). However, NzsG shows no homology to the identified bacterial or fungi aromatic or indole PTases. Further phylogenetic analysis indicated that NzsG forms the same branch with phytoene synthases instead of all of the known aromatic or indole PTases (Figure S4A), implying that NzsG may be a new type of emerging PTase family.

To determine the exact function of NzsG, we carried out a biochemical study. Overexpression of *nzsG* in *Escherichia coli* allowed isolation and purification of its encoded protein. The resultant NzsG appeared on SDS-PAGE with an estimated molecular weight of 38.1 kDa (Figure S4B). Incubations of the recombinant enzyme with dimethylallyl pyrophosphate (DMAPP) and **4** or **5**, supplemented with $Mg^{2+}$ (5 mM), were performed and the reactions monitored by HPLC. When the assays were conducted in the absence of DMAPP or in the presence of **4**, there was no turnover (Figure 4). Reactions with **5**, however, resulted in an efficient conversion of **5** to neocarazostatin B **2** as evidenced by the exact mass and co-elution time with the authentic sample of **2** (Figures 4A, 4B, and S4C), confirming that **5** is the key intermediate in the NZS biosynthesis but its *bis*-methylated derivative, **4**, is a shunt product in the Δ*nzsG* mutant (Figure 4). The enzyme was found to have optimal activity at pH 8.0 at 30°C in the presence of $Mg^{2+}$ (5 mM) ($K_M$ [**5**] = 202.5 ± 35.40, $k_{cat}$ = 0.052 ± 0.004 $min^{-1}$) (Figures S4D–S4F). There was no turnover when NzsG was incubated with DMAPP, farnesyl pyrophosphate, indole derivatives (e.g. L-tryptophan, indole 3-pyruvate), or other tricyclic molecules (e.g. carbazole, acridine,

**CellPress**

**Table 1. Deduced Functions of ORFs in *nzs* Biosynthetic Gene Cluster**

| Gene | Size[a] | Protein Homolog (Accession No.), Origin | I/S[b] | Proposed Function |
|---|---|---|---|---|
| *nzs*A | 418 | cytochrome P450 monooxygenase (NCBI: CBX53644), *Streptomyces platensis* NRRL 2364 | 34/51 | hydroxylation |
| *nzs*B | 355 | Anthranilate phosphoribosyltransferase (NCBI: AIR97966), *Streptomyces glaucescens* | 79/88 | tryptophan biosynthesis |
| *nzs*C | 185 | isopentenyl diphosphate delta-isomerase (NCBI: KES08965), *Streptomyces toyocaensis* | 72/77 | IPP isomerase |
| *nzs*D | 325 | phenylalanine aminotransferase (NCBI: AIR99319), *Streptomyces glaucescens* | 46/61 | aminotransferase |
| *nzs*E | 80 | acyl carrier protein (WP_030783257), *Streptomyces lavenduligriseus* | 62/77 | ACP |
| *nzs*F | 337 | FabH (NCBI: CAB62720), *Streptomyces coelicolor* A3(2) | 37/55 | KAS III |
| *nzs*G | 334 | phytoene synthase CrtB (NCBI: AAG28701), *Streptomyces griseus* IF013350 | 28/40 | isoprenyl transferase |
| *nzs*H | 593 | acetolactate synthase YerE (NCBI: AEP25490), *Yersinia pseudotuberculosis* | 27/41 | acetolactate synthase |
| *nzs*I | 227 | hypothetical protein (WP_030783270), *Streptomyces lavenduligriseus* | 80/88 | unknown function |
| *nzs*J | 331 | 3-oxoacyl-ACP synthase OleA (NCBI: ACS30828), *Micrococcus luteus* NCTC 2665 | 24/35 | KAS III |

[a]Amino acids.
[b]Identity/similarity.

fluorene, phenazine and dibenzothiophene, Figures 4, S4G–S4H), suggesting that NzsG has restricted substrate specificity. It has been demonstrated that some fungal indole PTases possess substrate promiscuity and can be used to prenylate larger aromatic ring systems, i.e. indolocarbazoles, using a chemoenzymatic approach (Yu et al., 2012). NzsG, however, is the first native carbazole PTase reported, and belongs to a new subgroup of aromatic PTases.

### Biochemical Assay Demonstrated that NzsA Is a P450 Hydroxylase Enzyme

Overexpression of *nzs*A in *E. coli* allowed isolation and purification of a soluble protein with an estimated molecular weight of 46.0 kDa, as observed in SDS-PAGE (Figure S5A). Carbon monoxide binding assay on NzsA monitored by UV spectroscopy demonstrated that NzsA is indeed a P450 enzyme (Figure S5B) (Meunier et al., 2004). In vitro experiments showed that the recombinant enzyme efficiently converted **2** into **1** (Figure S5C) in the presence of NADPH (see Supplemental Information). In control experiments, when assays were conducted in the absence of the NADPH or the enzyme NzsA or in the presence of **6**, there were no turnovers (Figure 5), confirming that NzsA catalyzes the installation of the hydroxyl group at C-11 position of **2** to yield **1**, and the epoxy derivative **6** is a shunt product in the ΔnzsA mutant. NzsA was also incubated with (*R*)-streptoverticillin **4** and precarazostatin **5**, but in both cases no formation of a new product, or disappearance of the starting material, was observed (Figure 5). These observations strongly suggest that NzsA mediates the last enzymatic step in the biosynthesis of **1**.

To further confirm the biotransformation from **5** to **1** in the NZS biosynthesis, in vitro reconstituted biotransformation was carried out. Upon incubation of **5** with the recombinant enzymes, NzsG and A, along with DMAPP, Mg²⁺, and NADPH (see Supple-mental Information), we observed the formation of **1** and **2** as evidenced by the exact mass and the same HPLC retention time as the authentic **1** and **2** (Figures S5D–S5E).

### DISCUSSION

Based on the bioinformatics analysis and the experimental data, we propose the biosynthetic pathway of **1** in MA37 as shown in Scheme 1. NzsB–F are likely to be involved in the precursor pathways. NzsB could be a housekeeping enzyme for tryptophan supply. NzsD resembles a family of PLP-dependent aromatic amino acid aminotransferases, suggesting its role in the conversion of L-tryptophan to indole-3-pyruvic acid. NzsC, a putative type I IPP isomerase, could be responsible for DMAPP supply (Berthelot et al., 2012). NzsE is a putative acyl carrier protein (ACP), which presumably transfers malonyl-coenzyme A (CoA) into malonyl-ACP. Both NzsF and NzsJ are annotated as putative 3-oxoacyl-ACP synthases (KASIII). However, they share no significant sequence similarity with each other. While NzsJ bears no significant homology to characterized KAS III proteins, NzsF shares moderate sequence identity (37% identity and 55% similarity) to FabH from *S. coelicolor* A3(2) (Revill et al., 2001), which catalyzes the condensation reaction between acetyl-CoA and malonyl-ACP to form acetoacetyl-ACP. It is postulated that NzsF is responsible for the formation of acetoacetyl-ACP using acetyl-CoA and malonyl-ACP as substrates, followed by reduction to generate 3-hydroxybutyryl-ACP.

We propose that NzsH could perform an acyloin coupling reaction between indole 3-pyruvate and pyruvate to generate α-ketoacid intermediate **7**. The condensation reaction between **7** and 3-hydroxybutyryl-ACP could be mediated by the putative KASIII enzyme NzsJ via a reversible indole attack to yield **8**. Decarboxylation-driven cyclization of **8** would result in an
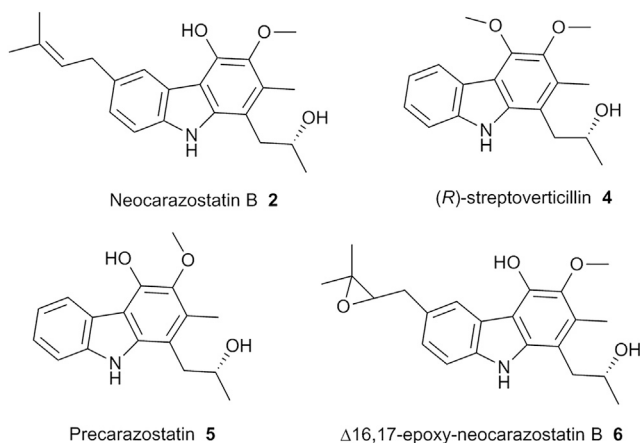
**Figure 3. Chemical Structures of Intermediates and Shunt Products Isolated from the Mutants in This Study**

The structures of **2**, **4**, **5**, and **6** were fully characterized by HR-ESIMS and 1D and 2D NMR spectroscopic analyses.

indole-fused cyclopentane intermediate **9**, which could immediately undergo the ring rearrangement to generate an indole-fused cyclohexanone tricyclic intermediate **10**, followed by dehydration and hydroxylation at C4 of **10**, to generate **11**. **11** would be readily tautomerized using positively charged nitrogen in the indole ring as the electron sink, followed by dehydration via base-catalyzed double-bond migration to furnish the *ortho*-quinone[*b*]indole tricyclic carbon backbone **12**. Examination of the metabolite profile extracted from the culture of the Δ*nzs*G mutant allowed identification of an ion with *m/z* identical to that of **12** (Figure S6). Although this compound could not be isolated, the mass is consistent with the structure of the predicted intermediate **12**. The enzyme(s) responsible for the formation of **12** remain to be confirmed. The formation of **12** may partially resemble the enzymatic reaction catalyzed by ScyC in the pathway of scytonemin (Balskus and Walsh, 2009). The dimeric alkaloid scytonemin is a cyanobacterial metabolite, functioning as a sunscreen (Balskus and Walsh, 2008). In the case of scytonemin biosynthesis, ScyA, a ThDP-dependent enzyme, was found to be responsible for the acyloin coupling of indole-3-pyruvate and *p*-hydroxyphenylpyruvate to yield the β-ketoacid product (Balskus and Walsh, 2008), which can then be cyclized and decarboxylated by the action of the unique enzyme, ScyC, to form the indole-fused cyclopentane intermediate (Balskus and Walsh, 2009). It is hypothesized that NzsI could play a key role in this multistep biotransformation, as our in vivo results indicated that *nzs*I is essential for the production of **1**. The exact roles of NzsH, J, and I in the biosynthesis of **1** is currently under investigation in our laboratories. **12** could further undergo reduction, followed by *O*-methylation, to yield the intermediate **5** and the shunt product streptovertillicin **4**. The prenylation event on **5** occurs in the presence of NzsG and DMAPP to produce **2**. The hydroxylation of **2** by NzsA finally provides **1**. Our in vivo and in vitro results unambiguously demonstrated the enzymatic coupled reactions from **5** to **1**, whereby the prenylation catalyzed by NzsG must occur prior to the NzsA-mediated hydroxylation (Figures 4 and 5). When *nzsA* is inactivated, the Δ*nzsA* mutant also accumulates the epoxylated metabolite **6** via an unidentified epoxidase.
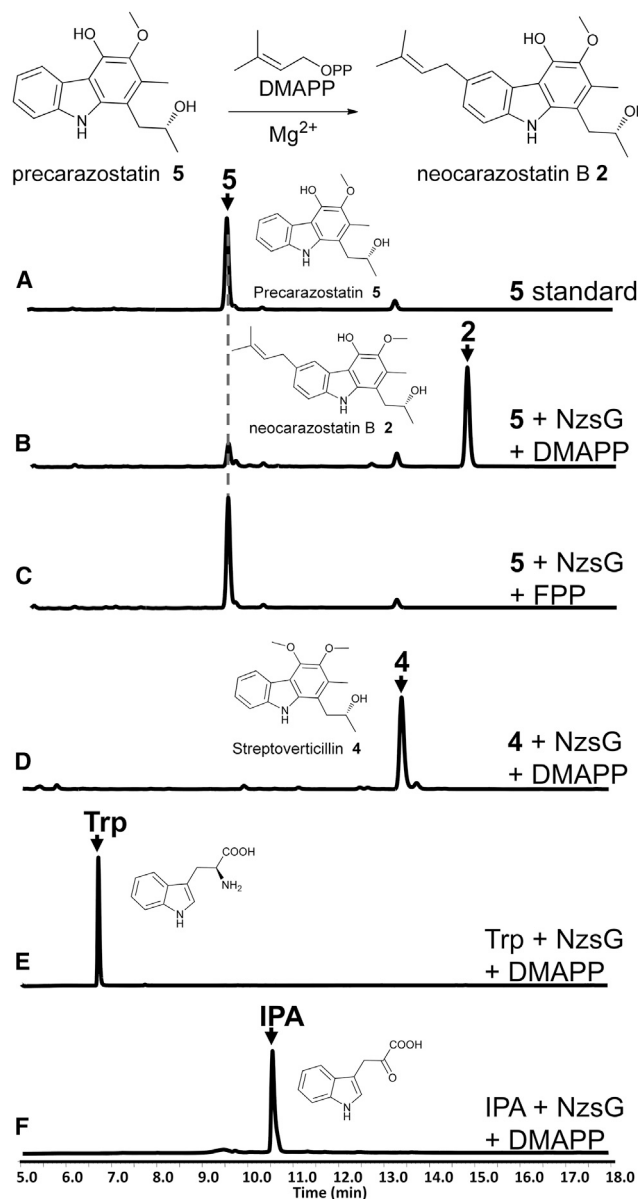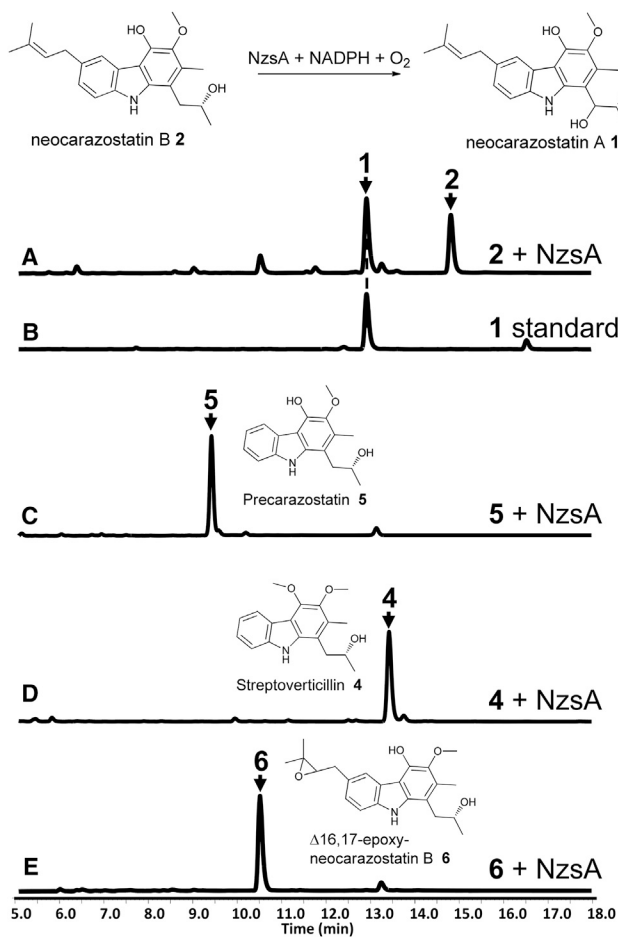


**Figure 4. HPLC Analysis of the Reactions Catalyzed by NzsG at UV of 247 nm**

Trace A shows the standard **5**. Trace B shows the analysis of the conversion of **5** to **2** in a reaction containing Mg²⁺ (5 mM), **5** (1 mM), NzsG (0.8 mg/ml), and DMAPP (0.2 mM); Traces C–F show the analyses of reactions containing Mg²⁺ (5 mM), NzsG (0.8 mg/ml), and various substrates, indicating that only **5** is the substrate for NzsG.

## SIGNIFICANCE

**Neocarazostatin A 1 is a potent free scavenging agent for protecting cell damage caused by free radicals. It possesses an intriguing tricyclic aromatic ring system, of which the chemical logic during the biosynthesis remains to be determined. We describe here the identification and characterization of the gene cluster for NZS biosynthesis in the soil bacterium *Streptomyces* sp. MA37 through in silico analysis,**

**Figure 5. HPLC Analysis of the Biochemical Reactions in the Presence of NzsA at UV of 247 nm**

Trace A shows the analysis of the conversion of **2** to **1** in a reaction containing **2** (1 mM), NzsA (1 mg/ml), spinach ferredoxin (100 μg/ml), spinach ferredoxin-NADP+ reductase (0.2 U/ml), NADPH (1.0 mM), glucose-6-phosphate (10 mM), and glucose-6-phosphate dehydrogenase (10 U/ml) in a Tris-HCl buffer (50 mM, pH 7.5). Trace B shows the standard **2**. Traces C–E show the analyses of reactions containing NADPH, NzsA (1 mg/ml) and various substrates, indicating that only **2** is the substrate for NzsA.

gene inactivation, and complementation. Biochemical assays of NzsG revealed that it is a new PSL-type carbazole prenyltransferase for NZS biosynthesis. In vitro assays confirmed that NzsA is responsible for the installation of a hydroxyl group at **2** to generate **1**. Finally, we reconstituted the last two reactions tailoring the NZS biosynthesis and demonstrated the sequential enzymatic reaction catalyzed by NszG, followed by NzsA to transform the key intermediate **5** to **1**.

## EXPERIMENTAL PROCEDURES

### Media and Strains

*E. coli* DH10B and *E. coli* ET12567 (pUZ802) were cultured in Luria-Bertani or Luria agar medium at 37°C. *Streptomyces* sp. MA37 was cultured in ISP2 medium (yeast extract 4 g/l, glucose 4 g/l, malt extract 10 g/l [pH 7.2]), and modified ISP4 medium (10 g/l soluble starch, 2 g/l $(NH_4)_2SO_4$, 1 g/l $K_2HPO_4$, 1 g/l

$MgSO_4 \cdot 7H_2O$, 1 g/l NaCl, 1 g/l tryptone, 0.5 g/l yeast extract, 1 g/l peptone, 1 ml/l trace element solution, adjusted pH to 7.2 before sterilization) containing the final concentration of 30 mM $Mg^{2+}$ was used for conjugation of *Streptomyces* sp. MA37.

### DNA Sequencing and Analysis

The ORFs of the *nzs* gene cluster were deduced from the sequence by running the FramePlot 4.0 beta program (http://nocardia.nih.go.jp/fp4/). The corresponding deduced proteins were compared with other known proteins in the databases using BLAST (http://www.ncbi.nlm.nih.gov/blast/). Amino acid sequence alignments were performed with the ClustalW algorithm from BIOLOGYWORKBENCH 3.2 software (http://workbench.sdsc.edu). The phylogenetic tree was drawn using MEGA 6.0 (Tamura et al., 2013). The sequence of the neocarazostatin biosynthetic gene cluster was identified from the sequenced genome via BLAST method using YerE as the sequence query. The neocarazostatins biosynthetic gene cluster was submitted to NCBI GenBank with the accession number NCBI: KP657980.

### Extraction and Purification of Neocarazostatin A, Neocarazostatin B, (*R*)-Streptoverticillin, Precarazostatin, and *16,17*-Epoxyneocarazostatin B

*Streptomyces* sp. MA37 and its mutants were inoculated into ISP2 medium, and were grown for 2 days at 28°C and 200 rpm. The culture was then transferred into fresh ISP2 medium (1:100, v/v) and cultivated at 28°C and 200 rpm for 5 days. Mycelia were collected and resuspended in one-tenth of the original culture volume of acetone, and the suspension was ultrasonically disrupted using a KQ3200V Ultrasonic cleaning apparatus (40 kHz, 25 min). Cell pellets were eliminated by centrifugation, and supernatants were subsequently dried out by rotary evaporation. Meanwhile the culture supernatant was extracted by an equal volume of ethyl acetate twice. The organic phase was collected and evaporated to dryness. Residues from two extracts were combined and redissolved in 1/100th of original culture volume of methanol for HPLC or liquid chromatography-mass spectrometry (LC-MS) detection. Purification of the target compounds was performed by gel filtration (Sephadex G200) using methanol as the mobile phase. The corresponding sections were dried by rotary evaporation and dissolved in methanol, and were further purified by semi-preparative HPLC on an Agilent ZORBAX SB-C18 column (5 mm, 9.4 × 250 mm) at a flow rate of 3 ml/min. The wavelength of the UV monitor was set at 247 nm. For the detection of neocarazostatin A, the mobile phase was 52:48 A/B (solvent A was 0.1% formic acid in ultrapure water and solvent B was 0.1% formic acid in $CH_3CN$); for neocarazostatin B, the mobile phase was 42:58 A/B; for (*R*)-streptoverticillin, the mobile phase was 45:55 A/B; for precarazostatin, the mobile phase was 53:47 A/B; and for *16,17*-epoxyneocarazostatin B, the mobile phase was 53:47 A/B. Finally, 10 mg of neocarazostatin A **1** ($[\alpha]^{19}_D$ −29 (c 0.07, MeOH)), 8.5 mg of neocarazostatin B **2** ($[\alpha]^{30}_D$ −28.8 (c 0.055, MeOH)), 7 mg of (*R*)-streptoverticillin **4** ($[\alpha]^{30}_D$ −18.4 (c 0.84 MeOH)), 4.3 mg of precarazostatin **5** ($[\alpha]^{31}_D$ −18.5 (c 0.07 MeOH)), and 4.5 mg of $\Delta^{16,17}$-epoxyneocarazostatin B **6** ($[\alpha]^{30}_D$ −30.5 (c 0.34, MeOH)) were obtained.

### HPLC and Tandem MS Analysis

HPLC analysis was carried out on a DIKMA Diamonsil C18 column (250 × 4.6 mm, 5 μm, column temperature 30°C) using a DIOEX P680 HPLC instrument. For fermentation analysis, samples were eluted with a gradient from 90:10 A/B to 60:40 A/B over 10 min, followed by another gradient to 45:55 A/B over 35 min at a flow rate of 1 ml/min, monitored by UV detection at 247 nm. For enzymatic analysis, samples were eluted with a gradient from 70:30 A/B to 0:100 A/B over 18 min, at a flow rate of 1 ml/min, and UV monitored at 247 nm. For carbazole, fluorene, phenazine, dibenzothiophene, acridine, Trp, IAA, IBA, and indole-3-pyruvic acid, samples were eluted with a gradient from 95:5 A/B to 0:100 A/B over 25 min, at a flow rate of 1 ml/min, and UV monitored at 220 nm for carbazole, fluorene, phenazine, dibenzothiophene, 392 nm for acridine, and 280 nm for Trp, IAA, IBA, and indole-3-pyruvic acid. Twenty percent of the eluent was injected to source and 80% to waste during LC-MS analysis. Solvent A was 0.1% formic acid in ultrapure water and solvent B was 0.1% formic acid in $CH_3CN$. The same column and LC gradient were used in all LC-MS analyses. High-resolution MS analysis, which consisted of a full scan in positive mode followed by a data-dependent
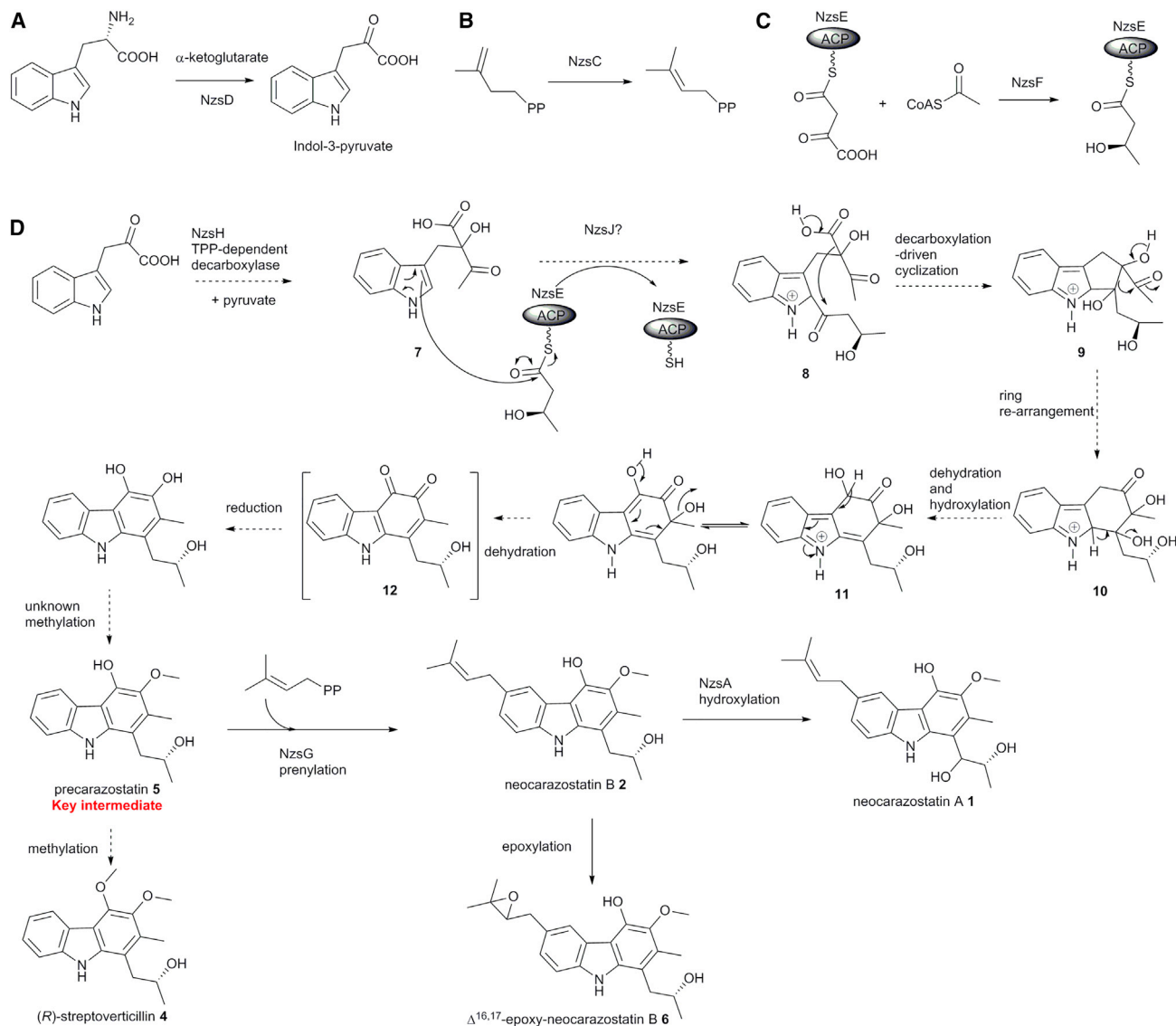
**Scheme 1. A Proposed Model for the Biosynthesis of NZS**

(A) Proposed model for indole-3-pyruvate.

(B) Biosynthesis of DMAPP.

(C) Biosynthesis of 3-hydroxy-butyryl-ACP.

(D) Proposed biosynthetic pathway of **1**. Bracket: **9** was observed to be present in the extract of the mutant Δ*nzsG* based on HR-ESIMS and MS$^n$ analyses. Dashed line: proposed reactions. Solid line: reactions were confirmed biochemically.

fragmentation scan, was performed on a Thermo Scientific LTQ XL Orbitrap mass spectrometer equipped with a Thermo Scientific Accela 600 pump.

### NMR Analysis

NMR spectra of neocarazostatin B **2** (8.5 mg), (*R*)-streptoverticillin **4** (7 mg), precarazostatin **5** (4.3 mg), and *16*,*17*-epoxyneocarazostatin B **6** were recorded on Agilent 600-MHz instrument in CD$_3$OD. NMR analyses of neocarazostatin A **1** were recorded on Varian 600-MHz spectrometer in CD$_3$Cl.

### Structural Elucidation of Neocarazostatin A 1

HR-ESIMS analysis of **1** established a molecular formula of C$_{22}$H$_{27}$NO$_4$. Dereplication using Antibase (Laatsch, 2013) suggested that this compound could be a known metabolite, neocarazostatin A, previously isolated from *Streptomyces* sp. GP38 (Kato et al., 1991). **1** also showed a characteristic UV pattern,

with absorption maxima at 229, 249, 271, 292, 331, and 345 nm. To confirm the structure, we obtained a complete set of 1D and 2D NMR spectral data. The structure of **1** was finally established through comparison of $^1$H and $^{13}$C NMR spectra data with those previously reported, which unambiguously confirms that **1** is neocarazostatin A.

### In-Frame Deletion of *nzsA* to *nzsH*

To inactivate *nzsA*, we amplified a 2,030-bp upstream fragment and a 2,002-bp downstream fragment from genomic DNA of *Streptomyces* sp. MA37 by PCR using the primers N-2-up-F/N-2-up-R and N-2-do-F/N-2-do-R, respectively (Table S3). PCR was performed in 20 μl volume with 5% DMSO and KOD DNA polymerase (Toyobo). The amplification conditions were: initial denaturation at 95°C for 5 min; 30 cycles of denaturation at 95°C for 30 s, annealing at 58°C for 30 s, and extension at 68°C for 2 min; and gap infilling at

**CellPress**

68°C for 10 min. The obtained fragments were cloned into the HindIII/EcoRI site of pKC1139 by using the In-fusion HD Cloning Kit (Clontech) to obtain the in-frame deletion vector construct, which was then transferred into *Streptomyces* sp. MA37 via *E. coli-Streptomyces* conjugation. Following a previously published procedure (Yu et al., 2009), the *nzsA* in-frame deletion mutant strains were identified by screening out and designated as WDY633. The same strategy was used to construct *nzsB* to *nzsJ* in-frame deletion mutants, except that different primers were used to amplify the left and right arms of the target genes (Table S3). The in-frame deletion mutant strains of *nzsB* to *NzsJ* were designated as WDY640, WDY641, WDY642, WDY644, WDY646, WDY638, WDY630, WDY648, and WDY635, respectively (Table S1).

### Complementation of the Mutant Strains WDY633, WDY644, WDY646, WDY638, WDY630, WDY648, and WDY635

To complement WDY633, a 1,257-bp fragment that contains the whole *nzsA* gene sequence was amplified from genomic DNA of *Streptomyces* sp. MA37 by high-fidelity PCR using the primers N-1-HB-F and N-1-HB-R (Table S3). The amplification conditions were: initial denaturation at 95°C for 5 min; 30 cycles of denaturation at 95°C for 30 s, annealing at 58°C for 30 s, and extension at 68°C for 1 min; and gap infilling at 68°C for 10 min. The obtained fragment was cloned into the NdeI/EcoRI site of pIB139, which can integrate into *Streptomyces* chromosome via the ΦC31 phage site. The construct obtained was then transferred into *Streptomyces* sp. MA37 in-frame deletion mutant via *E. coli-Streptomyces* conjugation. Following the procedure described previously (Kieser et al., 2000), the Δ*nzsA* complementation mutant strain was identified by screening out and designated as WDY634. The same strategy was used to complement WDY644, WDY646, WDY638, WDY630, WDY648, and WDY635, except that different pairs of primers were used for each complementation construct (Table S3). The complementation mutant strains of Δ*nzsE*, Δ*nzsF*, and Δ*nzsG–J* were identified by screening out and designated as WDY645, WDY647, WDY639, WDY631, WDY649, and WDY636, respectively.

### Construction of NzsA and NzsG Overexpression Vector

To overexpress NzsA, we amplified a 1,257-bp fragment that contains the whole *nzsA* from genomic DNA of *Streptomyces* sp. MA37 by PCR using the primers NzsA_F/NzsA_R (Table S2). PCR was performed in 20 μl volume with 5% DMSO and KOD DNA polymerase (Toyobo). The amplification conditions were: initial denaturation at 95°C for 5 min; 30 cycles of denaturation at 95°C for 30 s, annealing at 58°C for 30 s, and extension at 68°C for 90 s; and gap infilling at 68°C for 10 min. The obtained fragments were cloned into the KpnI/XhoI site of pHS_SUMO (Lv et al., 2015) using the In-fusion HD Cloning Kit (Clontech) to yield the overexpression construct pWDY651. The same strategy was used for *nzsG* cloning, except that the primers NzsG_F/NzsG_R were used for amplification (Table S3). The NzsG overexpression construct was designated pWDY650.

### Expression and Purification of NzsA and NzsG

The protein expression constructs pWDY638 and pWDY639 were individually transformed into *E. coli* BL21 (IDE3) (Novagen) competent cells. Single colonies from each transformation were inoculated to a starter culture (5 ml of super optimal broth [SOB] medium containing 50 μg/ml kanamycin) and cultivated at 37°C and 200 rpm. When the $A_{600}$ of the medium reached 0.5, the culture was transferred to 500 ml of fresh SOB medium and incubated at 37°C, 200 rpm. Isopropyl β-D-1-thiogalactopyranoside was added to a final concentration of 1 mM when the $A_{600}$ reached 0.6. After overnight culture at 16°C, cells were harvested by centrifugation and frozen at −40°C. All subsequent steps were performed at 4°C. After thawing on ice, cells were suspended in lysis buffer (200 mM Tris-HCl [pH 8.0], 500 mM NaCl, and 10 mM imidazole). The cell suspension was lysed with a Nano Homogenize Machine (AH100B; ATS Engineering). To separate the cellular debris from the soluble protein, the lysate was centrifuged at 20,000 × *g* at 4°C for 20 min. The supernatant was incubated with 1.5 ml Ni-Sepharose 6 Fast Flow (GE Healthcare) which had been pre-equilibrated with equilibration buffer (200 mM Tris-HCl [pH 8.0], 500 mM NaCl, and 10 mM imidazole) for 2 hr at 4°C. The resin was washed with 5 ml of the equilibration buffer, followed by twice washing with buffer containing 25 mM imidazole. The recombinant protein was eluted with 5 ml of wash buffer containing 250 mM imidazole. The eluted recombinant proteins were concentrated to 2.5 ml using Centrifugal Filter Units (Millipore

Regenerated Cellulose 3,000 molecular weight cutoff). The samples were then desalted by PD-10 Columns (GE Healthcare) according to the manufacturer's instruction. The cleavage of the SUMO tag of the eluted recombinant proteins was conducted using SUMO Protease (Invitrogen, catalog #12588-018) in buffer composed of 50 mM Tris-HCl (pH 8.0) and 150 mM NaCl at 4°C for 4 hr. The SUMO tag and SUMO Protease were finally removed from the cleavage reaction by using 0.5 ml of Ni-Sepharose 6 Fast Flow (GE Healthcare). The purified protein was stored at −80°C in storage buffer (50 mM Tris-HCl [pH 8.0], 150 mM NaCl, 10% [w/v] glycerol, and 1 mM DTT).

### NzsG Activity Assay

The enzyme assay of NzsG was carried out in 50 mM Tris-HCl buffer (pH 7.5) with 5 mM MgCl₂, containing 0.8 mg/ml NzsG, 1 mM substrate, and 0.2 mM DMAPP, in a final volume of 50 μl. The optimal assay conditions were obtained at 30°C. After 30 min, the reaction was quenched by the addition of two equal volumes of methanol and mixed by vortexing. The mixture was centrifuged at 15,000 rpm for 20 min to remove protein. The supernatant was then subjected to LC-tandem MS (MS/MS) analysis under the same conditions as described above.

### Kinetic Studies of NzsG

Optimization of NzsG in vitro assays is described in the legend of Figure S4D. The enzyme assays of NzsG were performed in a mixture (total volume 50 μl) containing 50 mM Tris-HCl (pH 8.0), 5 mM Mg²⁺, 1 mM DMAPP, 1 mM DTT, and 0.087–3 mM precarazostatin 5 at 30°C for 10 min. Reactions were initiated by the addition of enzyme (0.5 μM NzsG). An equal volume of methanol was added to quench the reaction and remove proteins by centrifugation. The supernatant was analyzed by HPLC. Kinetic analyses of NzsG reactions were carried out as described in the legend of Figure S4F.

### NzsA Activity Assay

Enzyme assay of NzsA activity was carried out on a 50-μl scale with substrates (1 mM), NzsA (1 mg/ml), spinach ferredoxin (100 μg/ml), spinach ferredoxin-NADP⁺ reductase (0.2 U/ml), NADPH (1.0 mM), glucose-6-phosphate (10 mM), and glucose-6-phosphate dehydrogenase (10 U/ml) in Tris-HCl buffer (50 mM, pH 7.5). After incubation at 30°C for 30 min, the reaction was quenched by the addition of two equal volumes of methanol and mixed by vortexing. The mixture was centrifuged at 15,000 rpm for 20 min to remove protein. The supernatant was then subjected to LC-MS/MS analysis under the same conditions as described above.

### ACCESSION NUMBERS

The sequence of the *nzs* gene cluster from *Streptomyces* sp. MA37 has been deposited in the GenBank database under the accession number NCBI: KP657980.

### SUPPLEMENTAL INFORMATION

Supplemental Information includes six figures and five tables and can be found with this article online at http://dx.doi.org/10.1016/j.chembiol.2015.10.012.

### ACKNOWLEDGMENTS

### REFERENCES

Aziz, R.K., Bartels, D., Best, A.A., DeJongh, M., Disz, T., Edwards, R.A., Formsma, K., Gerdes, S., Glass, E.M., and Kubal, M. (2008). The RAST

Server: rapid annotations using subsystems technology. BMC Genomics 9, 75.

Balskus, E.P., and Walsh, C.T. (2008). Investigating the initial steps in the biosynthesis of cyanobacterial sunscreen scytonemin. J. Am. Chem. Soc. 130, 15260–15261.

Balskus, E.P., and Walsh, C.T. (2009). An enzymatic cyclopentyl[b]indole formation involved in scytonemin biosynthesis. J. Am. Chem. Soc. 131, 14648–14649.

Baunach, M., Ding, L., Willing, K., and Hertweck, C. (2015). Bacterial synthesis of unusual sulfonamide and sulfone antibiotics by flavoenzyme-mediated sulfur dioxide capture. Angew. Chem. Int. Ed. Engl. 54, 13279–13283.

Berthelot, K., Estevez, Y., Deffieux, A., and Peruch, F. (2012). Isopentenyl diphosphate isomerase: a checkpoint to isoprenoid biosynthesis. Biochimie 94, 1621–1634.

Chen, H., Guo, Z., and Liu, H.-W. (1998). Biosynthesis of yersiniose: attachment of the two-carbon branched-chain is catalyzed by a thiamine pyrophosphate-dependent flavoprotein. J. Am. Chem. Soc. 120, 11796–11797.

Choshi, T., Sada, T., Fujimoto, H., Nagayama, C., Sugino, E., and Hibino, S. (1997). Total syntheses of carazostatin, hyellazole, and carbazoquinocins BF. J. Org. Chem. 62, 2535–2543.

Czerwonka, R., Reddy, K.R., Baum, E., and Knölker, H.-J. (2006). First enantioselective total synthesis of neocarazostatin B, determination of its absolute configuration and transformation into carquinostatin A. Chem. Commun. 711–713.

Deng, H., Ma, L., Bandaranayaka, N., Qin, Z., Mann, G., Kyeremeh, K., Yu, Y., Shepherd, T., Naismith, J.H., and O'Hagan, D. (2014). Identification of fluorinases from Streptomyces sp MA37, Norcardia brasiliensis, and Actinoplanes sp N902-109 by genome mining. ChemBioChem 15, 364–368.

Ding, L., Münch, J., Goerls, H., Maier, A., Fiebig, H.-H., Lin, W.-H., and Hertweck, C. (2010). Xiamycin, a pentacyclic indolosesquiterpene with selective anti-HIV activity from a bacterial mangrove endophyte. Bioorg. Med. Chem. Lett. 20, 6685–6687.

Ding, L., Maier, A., Fiebig, H.-H., Lin, W.-H., and Hertweck, C. (2011). A family of multicyclic indolosesquiterpenes from a bacterial endophyte. Org. Biomol. Chem. 9, 4029–4031.

Ellestad, G., Kunstmann, M., Lancaster, J., Mitscher, L., and Morton, G. (1967). Structures of methyl aldgarosides A and B obtained from the neutral macrolide antibiotic aldgamycin E. Tetrahedron 23, 3893–3902.

Feng, N., Ye, W.H., Wu, P., Huang, Y.C., Xie, H.H., and Wei, X.Y. (2007). Two new antifungal alkaloids produced by Streptoverticillium morookaense. J. Antibiot. 60, 179–183.

Howard-Jones, A.R., and Walsh, C.T. (2006). Staurosporine and rebeccamycin aglycones are assembled by the oxidative action of StaP, StaC, and RebC on chromopyrrolic acid. J. Am. Chem. Soc. 128, 12289–12298.

Huang, S., Tabudravu, J., Elsayed, S.S., Travert, J., Peace, D., Tong, M.H., Kyeremeh, K., Kelly, S.M., Trembleau, L., Ebel, R., et al. (2015). Discovery of a single monooxygenase that catalyzes carbamate formation and ring contraction in the biosynthesis of the legonmycins. Angew. Chem. Int. Ed. Engl. 54, 12697–12701.

Kaneda, M., Kitahara, T., Yamasaki, K., and Nakamura, S. (1990). Biosynthesis of carbazomycin-B .2. Origin of the whole carbon skeleton. J. Antibiot. 43, 1623–1626.

Kato, S., Kawai, H., Kawasaki, T., Toda, Y., Urata, T., and Hayakawa, Y. (1989). Studies on free radical scavenging substances from microorganisms. I. Carazostatin, a new free radical scavenger produced by Streptomyces chromofuscus DC 118. J. Antibiot. (Tokyo) 42, 1879–1881.

Kato, S., Shindo, K., Kataoka, Y., Yamagishi, Y., and Mochizuki, J. (1991). Studies on free radical scavenging substances from microorganisms. II. Neocarazostatins A, B and C, novel free radical scavengers. J. Antibiot. (Tokyo) 44, 903–907.

Kieser, T., Bibb, M.J., Buttner, M.J., Chater, K.F., and Hopwood, D.A. (2000). Practical Streptomyces Genetics (The John Innes Foundation).

Knölker, H.J., and Reddy, K.R. (2002). Isolation and synthesis of biologically active carbazole alkaloids. Chem. Rev. 102, 4303–4427.

Laatsch, H. (2013). AntiBase 2013: The Natural Compound Identifier (Wiley-VCH).

Lehwald, P., Richter, M., Röhr, C., Liu, H.w., and Müller, M. (2010). Enantioselective intermolecular aldehyde-ketone cross-coupling through an enzymatic carboligation reaction. Angew. Chem. Int. Ed. Engl. 49, 2389–2392.

Li, H., Zhang, Q., Li, S., Zhu, Y., Zhang, G., Zhang, H., Tian, X., Zhang, S., Ju, J., and Zhang, C. (2012). Identification and characterization of xiamycin A and oxiamycin gene cluster reveals an oxidative cyclization strategy tailoring indolosesquiterpene biosynthesis. J. Am. Chem. Soc. 134, 8996–9005.

Li, H., Sun, Y., Zhang, Q., Zhu, Y., Li, S.M., Li, A., and Zhang, C. (2015). Elucidating the cyclization cascades in xiamycin biosynthesis by substrate synthesis and enzyme characterizations. Org. Lett. 17, 306–309.

Liang, P.H., Ko, T.P., and Wang, A.H.J. (2002). Structure, mechanism and function of prenyltransferases. Eur. J. Biochem. 269, 3339–3354.

Lv, M., Zhao, J., Deng, Z., and Yu, Y. (2015). Characterization of the biosynthetic gene cluster for benzoxazole antibiotics A33853 reveals unusual assembly logic. Chem. Biol. 22, 1313–1324.

Ma, L., Bartholome, A., Tong, M.H., Qin, Z., Yu, Y., Shepherd, T., Kyeremeh, K., Deng, H., and O'Hagan, D. (2015). Identification of a fluorometabolite from Streptomyces sp. MA37:(2 R 3 S 4 S)-5-fluoro-2, 3, 4-trihydroxypentanoic acid. Chem. Sci. 6, 1414–1419.

Meksuriyen, D., and Cordell, G.A. (1988). Biosynthesis of Staurosporine, 1. $^1$H- and $^{13}$C-NMR assignments. J. Nat. Prod. 51, 884–892.

Meunier, B., De Visser, S.P., and Shaik, S. (2004). Mechanism of oxidation reactions catalyzed by cytochrome P450 enzymes. Chem. Rev. 104, 3947–3980.

Orihara, N., Furihata, K., and Seto, H. (1997). Studies on the biosynthesis of terpenoidal compounds produced by actinomycetes, 2. Biosynthesis of carquinostatin B via the non-mevalonate pathway in Streptomyces exfoliatus. J. Antibiot. 50, 979–981.

Palinski, W., Rosenfeld, M.E., Ylaherttuala, S., Gurtner, G.C., Socher, S.S., Butler, S.W., Parthasarathy, S., Carew, T.E., Steinberg, D., and Witztum, J.L. (1989). Low-density lipoprotein undergoes oxidative modification in vivo. Proc. Natl. Acad. Sci. USA 86, 1372–1376.

Pearce, C.J., Doyle, T.W., Forenza, S., Lam, K.S., and Schroeder, D.R. (1988). The biosynthetic origin of rebeccamycin. J. Nat. Prod. 51, 937–940.

Rawat, M., and Wulff, W.D. (2004). Total synthesis of carbazoquinocin C: application of the o-benzannulation of Fischer carbene complexes to carbazole-3,4-quinone alkaloids. Org. Lett. 6, 329–332.

Revill, W.P., Bibb, M.J., Scheu, A.K., Kieser, H.J., and Hopwood, D.A. (2001). Beta-ketoacyl acyl carrier protein synthase III (FabH) is essential for fatty acid biosynthesis in Streptomyces coelicolor A3(2). J. Bacteriol. 183, 3526–3530.

Ruanpanun, P., Dame, Z.T., Laatsch, H., and Lumyong, S. (2011). 3-Methoxy-2-methyl-carbazole-1,4-quinone, carbazomycins D and F from Streptomyces sp. CMU-JT005. FEMS Microbiol. Lett. 322, 77–81.

Sakano, K., and Nakamura, S. (1980). New antibiotics, carbazomycins A and B. II. Structural elucidation. J. Antibiot. (Tokyo) 33, 961–966.

Schmidt, A.W., Reddy, K.R., and Knölker, H.J. (2012). Occurrence, biogenesis, and synthesis of biologically active carbazole alkaloids. Chem. Rev. 112, 3193–3328.

Shin-ya, K., and Ogasawara, K. (1996). Enantiotopical synthesis of carbazoquinocins A and D, the potent lipid peroxidation inhibitors from Streptomyces violaceus 2448-SVT2. Synlett, 922–924.

Shin-ya, K., Tanaka, M., Furihata, K., Hayakawa, Y., and Seto, H. (1993). Structure of carquinostatin A, a new neuronal cell protecting substance produced by Streptomyces exfoliatus. Tetrahedron Lett. 34, 4943–4944.

Shin-ya, K., Kunigami, T., Kim, J.S., Furihata, K., Hayakawa, Y., and Seto, H. (1997). Carquinostatin B, a new neuronal cell-protecting substance produced by Streptomyces exfoliatus. Biosci. Biotechnol. Biochem. 61, 1768–1769.

Takada, K., Kajiwara, H., and Imamura, N. (2010). Oridamycins A and B, anti-Saprolegnia parasitica indolosesquiterpenes isolated from Streptomyces sp. KS84. J. Nat. Prod. 73, 698–701.

Takahashi, S., Takagi, H., Toyoda, A., Uramoto, M., Nogawa, T., Ueki, M., Sakaki, Y., and Osada, H. (2010). Biochemical characterization of a novel

**CellPress**

indole prenyltransferase from *Streptomyces* sp. SN-593. J. Bacteriol. *192*, 2839–2851.

Tamura, K., Stecher, G., Peterson, D., Filipski, A., and Kumar, S. (2013). MEGA6: molecular evolutionary genetics analysis version 6.0. Mol. Biol. Evol. *30*, 2725–2729.

Tanaka, M., Shin-ya, K., Furihata, K., and Seto, H. (1995). Isolation and structural elucidation of antioxidative substances, carbazoquinocins A to F. J. Antibiot. (Tokyo) *48*, 326–328.

Thomas, C., Kataeva, O., and Knölker, H.J. (2011). Transition metals in organic synthesis, part 96. First total synthesis of streptoverticillin: unambiguous confirmation of the absolute configuration. Synlett *18*, 2663–2666.

Wang, X., Tabudravu, J., Jaspars, M., and Deng, H. (2013). Tianchimycins A-B, 16-membered macrolides from the rare actinomycete *Saccharothrix xinjiangensis*. Tetrahedron *69*, 6060–6064.

Xu, Z., Baunach, M., Ding, L., and Hertweck, C. (2012). Bacterial synthesis of diverse indole terpene alkaloids by an unparalleled cyclization sequence. Angew. Chem. Int. Ed. Engl. *51*, 10293–10297.

Yamasaki, K., Kaneda, M., Watanabe, K., Ueki, Y., Ishimaru, K., Nakamura, S., Nomi, R., Yoshida, N., and Nakajima, T. (1983). New antibiotics, carbazomycin-A and carbazomycin-B. 3. Taxonomy and biosynthesis. J. Antibiot. *36*, 552–558.

Yu, Y., Duan, L., Zhang, Q., Liao, R., Ding, Y., Pan, H., Wendt-Pienkowski, E., Tang, G., Shen, B., and Liu, W. (2009). Nosiheptide biosynthesis featuring a unique indole side ring formation on the characteristic thiopeptide framework. ACS Chem. Biol. *4*, 855–864.

Yu, X., Liu, Y., Xie, X., Zheng, X.D., and Li, S.M. (2012). Biochemical characterization of indole prenyltransferases: filling the last gap of prenylation positions by a 5-dimethylallyltryptophan synthase from *Aspergillus clavatus*. J. Biol. Chem. *287*, 1371–1380.